A Robust and Efficient Block-Matching Framework for Non Linear Registration of Thoracic CT Images

Vincent Garcia[1], Olivier Commowick[2], and Grégoire Malandain[1]

[1] INRIA Sophia Antipolis – Méditerranée, Asclepios Team,
2004 route des lucioles, BP 93, 06902 Sophia Antipolis Cedex, France
[2] INRIA Rennes – Bretagne Atlantique, VISAGES Research Team,
Campus de Beaulieu, 35000 Rennes, France

Abstract. The registration of thoracic images is a challenging problem with essential clinical applications such as radiotherapy and diagnosis. In the context of the EMPIRE10 challenge, we briefly introduce a general robust and efficient algorithm to register automatically any type of scalar images (CT, MRI, ...) on virtually any location (brain, thorax, ...). Although fully automatic and generic, the proposed algorithm reached the 17^{th} place in the EMPIRE challenge over 34 algorithms evaluated. Moreover, we have since optimized further the parameter set used for the challenge and we demonstrate the ability of the algorithm to recover much better large displacements of the lungs boundaries.

1 Introduction

Registration of thoracic CT images is a challenging problem encountered in many clinical applications. For instance, one of the most important aspect in radiotherapy planning is to precisely determine the target volume to be treated and the surrounding critical structures. The elastic nature of the lung tissue deformation and the physiological movement of patient (e.g. breathing cycle) affects these localizations. Image registration may therefore greatly improve the treatment accuracy by compensating for the inevitable anatomical changes between two acquisitions.

To tackle this complicated registration problem, we propose a fully automatic non linear registration method, which may be applied to a large variety of medical images. It is based on a pyramidal block-matching approach, which allows to recover large displacements. To improve the robustness of the registration, the block-matching is coupled with an outlier rejection scheme to remove incorrect pairings that may occur due to several factors such as noise or lesions.

This algorithm was evaluated in the EMPIRE10 challenge, which provides a platform for in-depth evaluation and fair comparison of thoracic CT image registration algorithms. Although being generic and fully automatic, the proposed algorithm appears to be very efficient and competes with many state of the art registration methods specialized in thoracic CT image registration. Moreover,

since the evaluation results, better registration parameters were tested and we demonstrate the ability of our algorithm to recover much better large displacements of the lungs boundaries.

2 General Block-Matching Algorithm for Non Linear Registration

We developed a general algorithm to register a floating image F to a reference image R, i.e. find the dense transformation T (one displacement vector per voxel) so that F resampled by T locally matches R: $R \approx F \circ T$. Note that these reference and floating images may also be referred respectively as fixed and moving images in the literature. Our method is built on the principle of the block-matching based algorithm developed by Ourselin et al. for rigid registration [3]. However, its purpose is different and we therefore developed an algorithm to estimate a robust non linear transformation between the two images.

To compute this transformation, we follow an iterative framework using a multi-resolution scheme illustrated in Algorithm 1. At each iteration l, a transformation correction δT^l is evaluated using pairings obtained through block-matching, so that $F \circ T^l$ gets closer to R than $F \circ T^{l-1}$. As the block-matching algorithm may produce incorrect block pairings, the second step is then to detect and remove these outliers in order to compute an outlier-free transformation correction $\delta\tilde{T}^l$. Finally, the transformation correction is composed with the current transformation T^{l-1} to obtain T^l, which may be regularized using an elastic-like regularization scheme.

Algorithm 1 Block-Matching Based Non Linear Registration Algorithm

1: Initialize the transformation to identity $T^0 \leftarrow Id$.
2: **for** $p = 1...M$, iterations on pyramid levels, **do**
3: **for** $l = 1...L$, iterations, **do**
4: Estimation of pairings: $C \leftarrow \text{blockmatch}(R, F \circ T^{l-1})$.
5: Interpolate of a dense correction field: $\delta T^l \leftarrow \text{interp}(C)$.
6: Rejection of outlier pairings: $\tilde{C} \leftarrow \text{prune}(C, \delta T^l)$.
7: Interpolate the outlier free transformation correction: $\delta\tilde{T}^l \leftarrow \text{interp}(\tilde{C})$.
8: Composition of the correction $T^l = T^{l-1} \circ \delta\tilde{T}^l$.
9: Elastic-like regularization of the current transformation T^l.
10: **end for**
11: **end for**

2.1 Transformation Correction Estimation

At each iteration l, a dense correction field δT^l is computed to get a better correspondence between the images R and $F \circ T^{l-1}$. We detail in the following first how sparse pairings are obtained between the current images. Then, we present how this sparse information is used to compute a dense correction field.

Estimation of Correspondences To estimate correspondences between the images R and $F \circ T^{l-1}$, we have chosen to use a block-matching algorithm. It allows to search for large displacements between the images, while being robust to the possible local minima of the similarity measure.

Blocks are placed regularly on the whole reference image R. Then, for each block $B(x_v) \subset R$, centered in x_v, we look for its best match $B(y_v)$ in a local neighborhood $V(x_v) \subset F \circ T^{l-1}$ (this neighborhood can be small as we are working on an image pyramid). The best match is defined according to a similarity measure S, i.e. the best match is defined as :

$$y_v = \underset{y \in V(x_v) \subset F \circ T^{l-1}}{\arg\max} S(B(x_v), B(y)). \tag{1}$$

where $S(B(x_v), B(y))$ corresponds to the similarity measure between the two blocks $B(x_v)$ and $B(y)$. The choice of the similarity measure is crucial and must depend on the assumed relationship between the intensities of the two images. We have used small blocks in our experiments ($5 \times 5 \times 5$ voxels). This means that a small number of tissue classes are present in each block (usually two or three) [4], which fits perfectly the use of a squared correlation coefficient as a similarity measure.

We define S_v as the best value of the similarity measure for the block $B(x_v)$: $S_v = S(B(x_v), B(y_v))$. At the end of this step, we obtain a set of pairs of points (x_v, y_v) corresponding to the pairings between the images R and $F \circ T^{l-1}$. These pairs are associated to the corresponding values of the similarity measure S_v, that can be used for characterizing the confidence in each pairing.

Transformation Interpolation The obtained pairings can be seen as a sparse displacement field C, where each couple (x_v, y_v) implies the displacement $C(x_v) = y_v - x_v$. Similarly, a scalar sparse map of pairing confidence k may be built from the corresponding values S_v: $k(x_v) = S_v$.

The next step of the algorithm is then to interpolate a dense correction field from these two sparse fields. As we are estimating a dense non linear transformation, previous schemes (least squares) for linear transformation estimation may not be applied here. We therefore compute the dense transformation from the pairings by convolving C with a 3D Gaussian:

$$\delta T^l = \frac{G_\sigma * kC}{G_\sigma * k}. \tag{2}$$

The interpolation can be seen as a fluid regularization of the transformation as proposed in [2] in order to limit the influence of outliers. It is defined as a local mean of the pairings weighted by the confidence k to emphasize the pairings for which the confidence is high. This equation enables us to compute efficiently a dense correction field from the sparse displacement field C. σ corresponds to the standard deviation of the Gaussian, allowing to compute a smoother or sharper displacement field. Note that other methods could have been used to interpolate the dense correction field such as kriging [6] or thin-plate splines [1].

2.2 Outlier Rejection

From the block pairings, we have now obtained a dense correction field δT^l. However, the pairings obtained through the block-matching process may be erroneous in some regions such as regions where a lesion is present in one of the images, and in homogeneous regions. To prevent these outliers from corrupting the estimated transformation, we present an outlier rejection process. Unlike previous work on block-matching [3], our algorithm is designed for non linear registration, and techniques such as Least Trimmed Squares [5] may not be used. We therefore introduced an effective measure for the robust detection of outliers with respect to a non rigid transformation. We based our approach on the comparison of the original pairings (x_v, y_v) available in C and the interpolated displacements in δT^l. From this comparison, the mean displacement difference over the whole image e is computed as well as the variance σ_e^2:

$$\begin{cases} e &= \frac{1}{N}\sum_v \|C(x_v) - \delta T^l(x_v)\|, \\ \sigma_e^2 &= \frac{1}{N-1}\sum_v (e - \|C(x_v) - \delta T^l(x_v)\|)^2 \end{cases} \tag{3}$$

where N is the number of blocks in the image. Then, we define a criterion to determine whether a couple (x_v, y_v) is an outlier or not:

$$\|C(x_v) - \delta T^l(x_v)\| > e + \alpha\sigma_e. \tag{4}$$

In this equation, all the pairings whose difference with respect to the interpolated corrections field δT^l is higher than $e + \alpha\sigma_e$ are considered as outlier pairings and removed from the sparse field C. The α parameter allows more variable displacements when its value is large, and highly constrains the pairings when it is small. As with the LTS outlier rejection framework, this process could be iterated. However, only one iteration was sufficient to take into account the outliers and we therefore chose to use only one iteration.

After this outlier rejection step, the remaining pairings are used to compute a new sparse displacement field $\tilde{C}$, which is interpolated. This gives as a result a final correction field $\delta\tilde{T}^l$ that will be composed with the current transformation T^{l-1}: $T^l = T^{l-1} \circ \delta\tilde{T}^l$. Finally, the current estimate of the transformation T^l may be regularized using an elastic-like regularization, to provide a smoother deformation field. This amounts to convolve the current estimate T^l with a Gaussian kernel of standard deviation σ_{el}.

3 EMPIRE10 Challenge – Results

3.1 Challenge Context and Implementation Details

The EMPIRE10 challenge consisted in evaluating the state of the art in chest CT registration. 20 pairs of chest CT scans (intra-subject) had to be registered. The provided data were very challenging since they encompassed many of the problems faced by researchers developing registration algorithms for this application (variation in image/voxel size, scans taken at various phases in the breathing

cycle, etc.). In addition to the CT scans, binary lung masks were also provided for each pair of scans. The reader may find the proposed registration method referenced as "Asclepios2" in the EMPIRE10 challenge.

The implementation used for the challenge was done in C++. To register each pair of images, we first performed a global affine registration between the reference and floating images using the method proposed by Ourselin et al. [3]. As explained in Section 2, this method is also based on a block-matching scheme. It is able to estimate a linear transformation (rigid or affine) between two images. In this paper, we used the affine version of the method. The parameters used for the challenge was:

- Number of pyramid level: 4
- Number of iteration at each level: 6
- Type of estimator: weighted least trimmed squares

The value of other parameters was set by default. This first registration allowed to compensate for the global deformation induced by change in position of the patient or by the lung position in the breathing cycle. To focus on the lung part, the affine registration was performed on the masked images. The resulting affine transformation was then given as an initial transformation to our non linear registration algorithm. The parameter set used to register (non linear registration) each couple of images was:

- Number of pyramid levels: 4
- Size of blocks: $5\times5\times5$
- Search window size: $7\times7\times7$
- Number of iterations per pyramid level: 10

We found that the impact of the last pyramid level (finest resolution) brought only negligible registration quality improvement in comparison to the computation time increase. The last level of pyramid was therefore skipped in order to speed-up the computation. To further decrease computation time and since only the lungs registration was evaluated, we also decided to use the lung mask of the reference image to define blocks only where needed in the reference image. Since the parameters used are the same for every pair of scans, the method is considered as fully automatic.

3.2 Numerical Results

Table 1 and Fig. 1 present the results of the EMPIRE10 challenge for the proposed registration method. For each pair of images, the registration method was evaluated by four criteria:

- Alignment of lung boundaries
- Alignment of major fissures
- Correspondence of annotated point pairs

– Analysis of singularities in the deformation field

Overall, the proposed registration method appeared to be a very efficient method for thoracic CT images with a rank of 17 among the 34 competing algorithms. Three major conclusions may be drawn. First, the proposed method obtains a perfect score on singularities in the deformation field. This comes both from the outlier rejection scheme and from the interpolation of sparse displacement fields over the whole image. This allows our algorithm to compute deformation fields with no singularities. Second, our method is very efficient to align the fissures and landmarks, ranking at the 13^{th} place in average for this evaluation. Finally, the alignment of the lung boundaries does not perform as well as we had expected for some scan pairs. This issue comes from the fact that we adapted the parameters from a set that was designed for brain registration, where displacements are much smaller. We since investigated this problem and

	Lung Boundaries		**Fissures**		**Landmarks**		**Singularities**	
Scan Pair	**Score**	**Rank**	**Score**	**Rank**	**Score**	**Rank**	**Score**	**Rank**
01	0.85	28.00	0.54	18.00	2.41	12.00	0.00	11.50
02	0.00	30.00	0.00	15.00	0.62	25.00	0.00	12.50
03	0.00	28.00	0.00	12.50	0.65	23.00	0.00	12.00
04	0.00	12.00	0.00	16.50	0.92	7.00	0.00	14.00
05	0.00	13.00	0.00	16.00	0.71	30.00	0.00	13.50
06	0.00	16.00	0.00	15.00	0.47	26.00	0.00	14.00
07	2.50	29.00	0.93	14.00	1.85	7.00	0.00	10.00
08	0.09	28.00	0.00	12.00	1.02	15.00	0.00	12.50
09	0.00	24.00	0.00	6.50	0.71	21.00	0.00	13.00
10	0.01	22.00	0.00	15.00	1.17	7.00	0.00	13.50
11	0.78	29.00	0.01	11.00	1.02	12.00	0.00	11.50
12	0.07	31.00	0.00	27.00	0.94	28.00	0.00	14.50
13	0.03	32.00	0.08	13.00	1.19	20.00	0.00	13.00
14	0.48	27.00	2.78	9.00	1.78	5.00	0.00	9.50
15	0.00	23.00	0.00	7.00	0.81	23.00	0.00	12.50
16	0.00	30.00	0.03	11.00	1.23	17.00	0.00	13.50
17	0.00	22.00	0.05	16.00	1.18	24.00	0.00	14.00
18	0.91	28.00	0.09	5.00	1.55	5.00	0.00	10.50
19	0.00	14.00	0.00	12.00	0.66	26.00	0.00	14.50
20	0.18	25.00	2.69	15.00	1.64	9.00	0.00	10.50
Avg	0.29	24.55	0.36	13.32	1.13	17.10	0.00	12.52
Average Ranking Overall								16.87
Final Placement								17

Table 1. Results for each scan pair, per category and overall. Rankings and final placement are from a total of 34 competing algorithms.

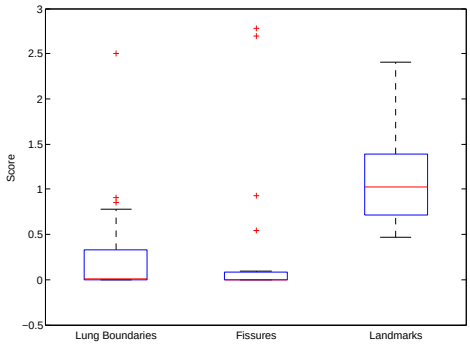

Fig. 1. Scores of the proposed registration method: box-and-whisker plot for categories "lung boundaries", "fissures", and "landmarks". Information about "singularities" were not displayed since the score was 0 for every scan pair.

propose in Section 3.4 a simple modification of the parameter set that settles the boundary precision problem while improving the global registration quality.

3.3 Visual Results

In this section, we present some visual results illustrating the performance of our method. The presented images correspond to axial slices of the lungs. In order to focus the reader attention onto the lungs, the contrast in these regions has been artificially increased while the contrast outside has been decreased. This manipulation on the contrast was possible thanks to the masks provided for both reference and floating images. Since the registered image is supposed to perfectly match the reference image, the contrast change of the registered image has been performed using the mask of the reference image. As a consequence, a misalignment of the lung boundary will appear as a thin white band in the lung mask and as a dark band outside of the mask.

According to Table 1, the registration process using the proposed set of parameters was particularly efficient on the pairs of scans #2 and #19. Fig. 2 illustrates for both scan pairs, respectively from left to right, the floating image, the registered image, and the reference images. One can see that the initial data (reference and floating images) are clearly not registered (lung boundaries, vessels, bronchus, etc.). Using our algorithm, the registered image appears to be very similar to the reference image: the lung boundaries are correct and most of the structures in the reference image are present and well positioned in the registered image.

According to Table 1, our algorithm is however less efficient on the scan pairs #1 and #18 (see Fig.3). One can notice that the lung boundaries have not been retrieved as precisely as we expected. However, inside the lungs, the two registered images are very similar to their corresponding reference images. The proposed method is therefore reliable and allows to precisely compare visually the reference and registered floating images.

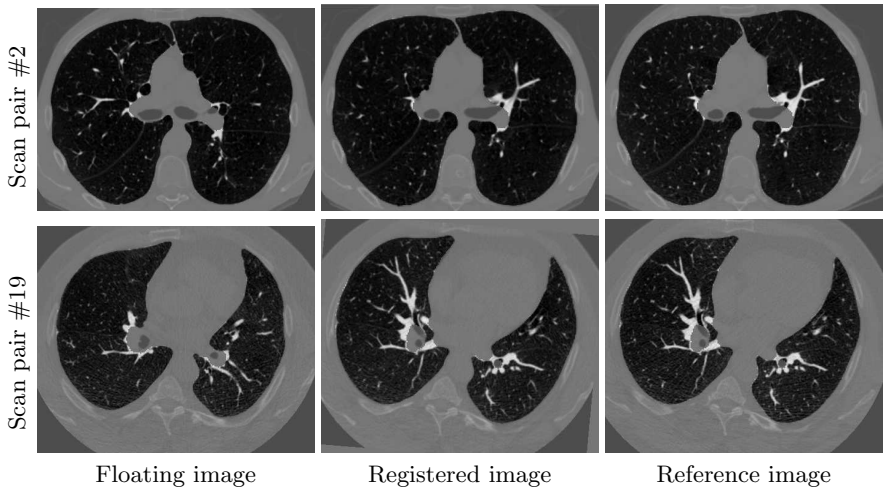

Fig. 2. Image registration results (two of the most accurate examples according to Table 1). The registered image (central column) is the floating image (left column) re-sampled in the geometry of the reference image (right column). Slice numbers are 317 for the scan pair #2, and 194 for the scan pair #19.

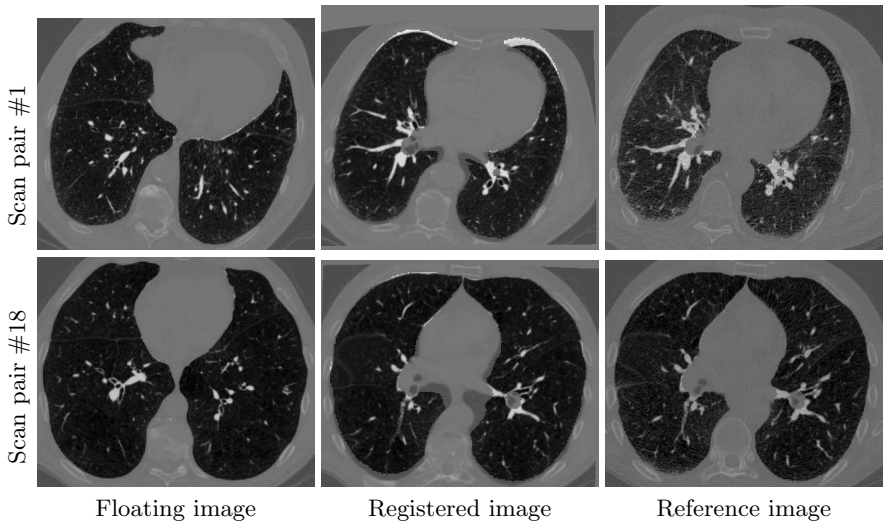

Fig. 3. Image registration results (two of the less accurate examples according to Table 1). Slice numbers are 148 for the scan pair #1, and 170 for the scan pair #18.

3.4 Improvements

Thanks to the results of the evaluation, the boundary alignment issue, illustrated in Fig. 3, was detected. As mentioned above, this comes from the fact that we adapted the parameter set used in the experiments from one used for

brain registration. However, the displacements encountered in brain registration are much smaller than in lung registration.
Since the submission of the results, we further improved the parameters and found a single set of parameters allowing for a much better visual correspondence of the lung boundaries. This improvement resides in two changes. First, we increased the number of iterations per pyramid level to 15 to ensure that all displacements are recovered. Then, we gave the algorithm a dilated mask of the lungs as the area on which to create blocks. This was done to ensure that blocks are created on the border of the lungs, allowing for their precise registration.
Fig. 4 illustrates the improvement between the two sets of parameters. The new set of parameters visually corrects the lung boundary matching issue. In addition, the alignment of fissures also seems to be improved: some fissures visible in the reference image were lost in the registered image with the submitted method and are well recovered using the improved registration method.

3.5 Computation time

The computation time of a given registration method depends mainly on the hardware configuration of the computer used. For our experiments, the configuration was the following: DELL laptop E6400, CPU double core at 2400MHz, 8GB of DDR3 memory, Linux Fedora 10. Using this configuration, and using the set of parameters of the initial submission, the computation time was distributed between the affine registration and the non linear registration:

– Affine registration: 123 seconds

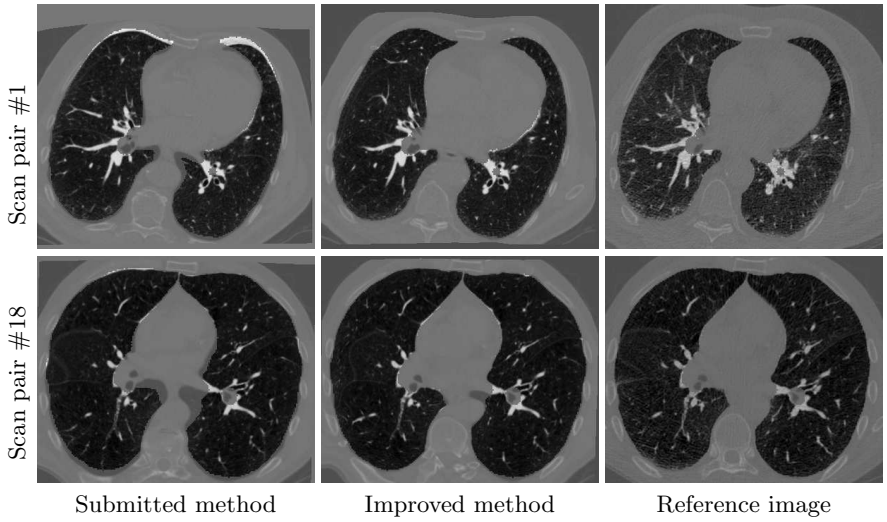

Fig. 4. Improvement of the proposed registration method. The lung boundary issue has been fixed. The slice numbers are 148 for the scan pair #1, and 170 for the scan pair #18.

– Non linear registration: 623 seconds

These computation time was obtained for the image #1. Using the improved set of parameters, the computation time of the non linear registration slightly increased and was, on the same image, 844 seconds. One should note that the code can be distributed on a multiple core architecture. In order to compare the distribution of the computation time between the linear and the non linear registration processes, we used one of the two cores available. Indeed, the affine registration was optimized for single core processors.

4 Conclusion

The registration of thoracic images is a challenging problem having critical clinical applications such as radiotherapy and diagnosis. In this context, the EMPIRE10 challenge had a simple but essential goal: objectively compare the thoracic CT image registration algorithms proposed by the research community.

In this paper, we introduced an efficient algorithm to register automatically any type of scalar images on a large variety of locations. Associated to an outlier rejection scheme, this method is also robust to incorrect pairings that may occur. Although fully automatic and generic, our algorithm performed well and reached the 17^{th} place in the challenge over 34 algorithms evaluated. Moreover, we presented a new set of parameters that drastically improves the visual results compared to the challenge results, allowing to recover much better large displacements of the lungs boundaries.

Finally, this method is currently being integrated into the MedINRIA software platform[3] to make it available to clinicians and researchers.

References

1. Bookstein, F.L.: Principal warps: Thin-plate splines and the decomposition of deformations. IEEE TPAMI 11(6), 567–585 (1989)
2. Christensen, G.E., Rabbitt, R.D., Miller, M.I.: Deformable templates using large deformation kinematics. IEEE TIP 5(10), 1435–1447 (1996)
3. Ourselin, S., Roche, A., Prima, S., Ayache, N.: Block matching: A general framework to improve robustness of rigid registration of medical images. In: MICCAI '00. LNCS, vol. 1935, pp. 557–566 (2000)
4. Roche, A., Malandain, G., Ayache, N.: Unifying maximum likelihood approaches in medical image registration. Int. Journal of Imaging Systems and Technology: Special Issue on 3D Imaging 11(1), 71–80 (2000)
5. Rousseeuw, P., Leroy, A.: Robust Regression and Outlier Detection. John Wiley and Sons, Inc., New York, NY (1987)
6. Ruiz-Alzola, J., Westin, C.F., Warfield, S.K., Alberola, C., Maier, S., Kikinis, R.: Nonrigid registration of 3D tensor medical data. MedIA 6(2), 143–161 (2002)

[3] http://www-sop.inria.fr/asclepios/software/MedINRIA/